Pergamon

Journal of Structural Geology, Vol. 16, No. 2, pp. 237 to 252, 1994
Elsevier Science Ltd
Printed in Great Britain
0191-8141/94 $06.00+0.00

Interference between pluton expansion and coaxial tectonic deformation: three-dimensional computer model and field implications

GIOVANNI GUGLIELMO, JR

Bureau of Economic Geology, University of Texas at Austin, Austin, TX 78713-7508, U.S.A.

(*Received* 8 *June* 1992; *accepted in revised form* 12 *March* 1993)

Abstract—Structures in orogenic belts are greatly controlled by interactions between pluton-related and tectonic-related strain fields. However, many aspects of the geometry and evolution of these structures are poorly known. For example, (1) What is the geometry of these structures if regional deformation is coaxial? (2) How does this geometry change with progressive deformation? This paper describes a three-dimensional simulation of strain shape and magnitude as well as foliation and lineation patterns formed by interactions between pluton expansion and homogeneous coaxial deformation.

This simulation suggests that interactions between pluton expansion and regional uniaxial shortening generate patterns that are distinct from the patterns produced by regional uniaxial extension or regional non-coaxial deformation. For example: shortening produces doughnut-shaped constrictional rings about the pluton, whereas extension produces apple-shaped flattening regions around the pluton. In addition, shortening produces one continuous doughnut-shaped low-strain region around the pluton. On the other hand, extension creates two separate ellipsoidal low-strain regions at the ends of the pluton. Furthermore, shortening forms foliation rings that have triangular two-dimensional sections, and lineation is concentric around the axis of maximum shortening. In contrast, extension produces two separate foliation and lineation cones at the ends of the pluton. All these structural and strain elements migrate away from the pluton with increasing expansion rates and towards the pluton with increasing tectonic deformation rates.

Although structural studies around plutons should always integrate microstructural, radiometric and field measurements, simulation-generated patterns can be used to evaluate: (1) origin, geometry and evolution of structures around plutons; (2) mechanisms that explain inclusion trails within porphyroblasts; (3) contribution of pluton-related strains to strains measured in the country rock; and (4) type and three-dimensional orientation of regional kinematic schemes.

INTRODUCTION

THE geometry of structures around plutons controls the shape and size of hydrothermal ore deposits associated with granites. In addition, structures around plutons are used to estimate width of strain aureoles, which may, in turn, provide room required for pluton emplacement (Paterson & Fowler 1993 and references therein). Furthermore, cross-cutting relationships between aureole structures and plutons of known age are often used to determine the age of these structures.

Structures in country rocks are produced by the interplay of many processes including: (1) stoping (Daly 1903, 1933, Goodchild 1982); (2) thermal shattering (Daly 1903, Roberts 1970, Koide & Bhattacharji 1975, Marsh 1982); (3) partial melting and anatexis (Holmes 1965, Ahren *et al.* 1980, Huppert & Sparks 1988, Bergantz 1989); (4) diapiric rise of the pluton (Berner *et al.* 1972, Ramberg 1972, Coward 1981, Schwerdtner 1981, Marsh 1982, Van Den Eeckhout & Vissers 1986, Jackson & Talbot 1989 and many others); (5) regional deformation before, during and after pluton emplacement (Castro 1986, Dimroth *et al.* 1986, Tobisch *et al.* 1986, Hutton 1988); and (6) pluton expansion (Ledru & Brun 1977, Sylvester *et al.* 1978, Brun & Pons 1981, Holder 1981, Bateman 1985, Castro 1986, Ramsay 1989, Brun *et al.* 1990, Morgan *et al.* 1991, Corriveau 1992, Seltmann & Bankwitz 1992). All these processes contribute to the complexity of structures in strain aureoles. However, physical and computer simulations allow the study of individual geological processes separately, which clarifies cause–effect relationships. Therefore, although simulations are necessarily simplifications of nature, they aid in understanding the genesis of structures around plutons.

Many simulations quantify strain patterns around plutons (Dixon 1975, Schwerdtner & Troeng 1978, Morgan 1980, Brun & Pons 1981, Cruden 1988, Schmeling *et al.* 1988, Mandal & Chakraborty 1990). However, few studies used computer models to examine strain patterns around expanding plutons subjected to tectonic deformation in either two dimensions (Brun & Pons 1981, Mandal & Chakraborty 1990) or three dimensions (Guglielmo 1993b). Whereas Guglielmo (1993b) simulates non-coaxial regional deformation, the present paper studies pluton expansion in a coaxial environment.

This paper suggests: (1) how three-dimensional strain and structural patterns formed around a pluton that expands during uniaxial shortening and uniaxial extension change with progressive deformation; (2) that ordinary geological processes can explain complex inclusion trails within porphyroblasts; and (3) that strain patterns around expanding plutons, when used in conjunction with mesoscopic and microscopic kinematic

indicators, can help to establish the orientation of end-member regional kinematic schemes in three dimensions.

APPROACH TO MODELING

This kinematic simulation assumes that a spherical pluton expands radially, and produces concentric flattening strain ellipsoids with intensities that decrease away from the pluton. These strains were modeled based on strains measured around natural plutons (Sanderson & Meneilly 1981, Guglielmo 1993a) and physical and computer models (Dixon 1975, Cruden 1988, Schmeling *et al.* 1988). Homogeneous uniaxial tectonic deformation is described by the tensor

$$P = \begin{vmatrix} pB & 0 & 0 \\ 0 & \frac{1}{\sqrt{p}}B & 0 \\ 0 & 0 & \frac{1}{\sqrt{p}}B \end{vmatrix},$$

where B is the expansion material rate (Brun & Pons 1981, Guglielmo 1993b) and p is the pure shear material rate. p values smaller than 1 represent uniaxial shortening, whereas p values greater than 1 represent uniaxial extension.

At each iteration of the program, wall rock particles are displaced according to the tensor described above. The simulation considers expansion before, during and after coaxial ductile deformation, as well as the effects of variations in tectonic and expansion rates. Strains are visualized in three dimensions using four strain parameters: strain ellipsoid shape, magnitude as well as orientation of foliation and mineral stretching lineations. The simulation is interactive which allows changes in parameters of strain tensors (strain rates) *during* the simulation and display and evaluation of resulting strain patterns in real time. Computer graphics and programming aspects of this simulation are described by Guglielmo (1992), whereas mathematical proofs are given by Guglielmo (1993b).

RESULTS

During pluton expansion in an uniaxial shortening environment, the pluton assumes a three-dimensional ellipsoid (pancake) shape whose minor axis is parallel to the shortening direction (Fig. 1). Conversely, during pluton expansion in a uniaxial extensional tectonic environment, the pluton assumes an ellipsoid (cigar) shape whose major axis is parallel to the extension direction (Fig. 2). Although distinct regional kinematic schemes produce distinct pluton shapes, the definition of the words 'ends' and 'sides' of the pluton (Guglielmo 1993b) are independent of these kinematic schemes, shapes or 'way-up' direction. Throughout this paper the word 'ends' refers to the regions in the country rock near the plutons where the pluton–wall rock contact has the sharpest curvature. Conversely, 'sides' refer to regions in the wall rock where the contact has the lowest curvature (Figs. 3a & c).

During pluton expansion in a coaxial tectonic environment 'ends' and 'sides' of the pluton are subjected to distinct interferences between pluton-related and tectonic-related strain fields. The nature of this interference controls the strain ellipsoid magnitude, shape, and orientation, which in turn control the intensity, type and geometry of structures around the pluton. The three-dimensional geometry of these structures and how this geometry changes during progressive coaxial deformation have not been previously described.

Strain shape patterns

Strain shape patterns control the types of structures around the pluton. Regions of high constriction favor conspicuous mineral stretching lineations. Conversely, in regions of high flattening, foliation development would predominate over stretching lineations.

Shortening. During pluton expansion in a uniaxial shortening environment, a three-dimensional doughnut-shaped surface separates areas of constriction from areas of flattening (green surface around the pluton in Fig. 1i). Regions of constriction are within the doughnut at the ends of the pluton, whereas regions of flattening occur at the sides of the pluton (Fig. 1i).

Absolute values of strain ellipsoid parameters are used to plot the more useful qualitative strain patterns (e.g. high constrictional regions vs low constrictional regions, etc.). Lode's parameter (Lode 1926) absolute values are shown in a two-dimensional slice (Fig. 1c) through the center of the pluton (Fig. 1i). This slice is parallel to the plane of the paper. The green surface (Fig. 1i) connects all points in three-dimensional space that have Lode's parameter equal to zero. This surface corresponds to the boundary between the green and yellow areas in the two-dimensional slice (Fig. 1c). Between the pluton and the green surface (Fig. 1i), Lode's parameter is between 0 and 1, corresponding to the yellow, red and pink areas in the two-dimensional slice. Finally, in the region within the doughnut at the ends of the pluton (Fig. 1i), Lode's parameter is between 0 and -1, which corresponds to green and blue areas in the two-dimensional slice. The highest constrictional strains in the area occur within the pink surface (Fig. 1i). This surface corresponds to the blue constrictional point in the two-dimensional slice (Fig. 1c).

During progressive syntectonic deformation, constrictional rings approach the pluton (cf. Figs. 1c & g). Real-time simulations show that rates of ring migration are much slower than either rates of tectonic defor-

mation or pluton expansion. Slow ring migration can also be documented by comparing initial and final strain patterns. For example, distances between ring and pluton changed little when compared with displacements caused by tectonic deformation (Figs. 1c & g), suggesting slow ring migration rates.

During progressive deformation, changing the rates of pluton expansion relative to tectonic deformation affects the size and position of constrictional regions. Higher expansion rates relative to tectonic deformation rates increase the size of constrictional regions and displace them away from the pluton (cf. Figs. 1j & k). Conversely, higher tectonic rates relative to expansion rates make regions of constriction smaller and closer to the pluton.

Extension. During pluton expansion in a uniaxial extensional environment, a three-dimensional apple-shaped symmetric surface (pink surface around the pluton in Fig. 2i) separates regions of constriction from regions of flattening. Regions of flattening are around and in direct contact with the pluton. This three-dimensional region of flattening is analogous to the edible portion of an apple, where the pluton would represent the 'core' (Figs. 2c, g, i & k). Regions of constriction also ring the pluton. During most of the deformation history (see below), however, they are not in contact with the pluton. Constrictional strains occur close to the pluton at its ends (bottom and top of apple), and far from the pluton at its sides (Figs. 2c, g, i & k). Lastly, an isotropic point (strain magnitude equal to zero) forms at each the end of the pluton (Fig. 2gI).

Lode's parameter absolute values are shown in a two-dimensional slice (Fig. 2g) cut through the center and ends of the three-dimensional pluton (Fig. 2i). The pink surface (Fig. 2i), where Lode's parameter equals zero, corresponds to the boundary between the yellow and green areas in the two-dimensional slice (Fig. 2g). Between the pluton and the pink surface, Lode's parameter is between 0 and 1. This region corresponds to the yellow, red and pink areas in the two-dimensional slice. Along the green surface (Fig. 2i) Lode's parameter equals -0.3, corresponding to the boundary between the green and light blue areas in the two-dimensional slice. Finally, outside the blue surface, Lode's parameter values are between -0.5 and -1. This region approximately corresponds to the dark blue areas in the two-dimensional slice.

During progressive deformation, changing the rates of pluton expansion with respect to tectonic deformation changes the size and position, but not the shape, of flattening and constrictional regions. Higher expansion rates relative to tectonic deformation rates increase the size of flattening regions and consequently displace constrictional regions and isotropic points away from the pluton. Conversely, higher tectonic rates relative to expansion rates makes regions of flattening smaller and closer to the pluton. At very high tectonic rates, regions of constriction may touch the ends of the pluton. In addition, the movement of flattening and constriction regions occurs at rates that are much slower than rates of tectonic deformation or pluton expansion.

Strain magnitude patterns

Strain magnitude patterns control the intensities of fabric and structures around the pluton. In regions of high strains, foliations and lineations are conspicuous and easier to measure. In addition, high strains favor resetting of quartz fabrics and other microstructures. Conversely, in low-strain zones, structures are less developed and structures formed during previous deformation events have a better chance of surviving subsequent deformation.

Shortening. During pluton expansion in a uniaxial shortening environment, low-strain zones have the shape of a toroid around the ends of the pluton (Fig. 1m). On the other hand, regions of high strains assume a three-dimensional convex lens shape (Fig. 1n) in each side of the pluton. Comparing the pluton with a car wheel, the tire would represent low-strain zones and the hub caps would represent regions of high strains.

Strain magnitude absolute values are shown in a two-dimensional slice (Fig. 1e) through the center of the three-dimensional pluton (Figs. 1m & n). Within the three-dimensional low-strain toroid (Fig. 1m) strain magnitudes are lower than 1.0, and correspond approximately to the light blue area in the two-dimensional slice (Fig. 1e). On the other hand, within the high strain 'hub caps' (Fig. 1n) strain magnitudes are higher than 1.5, and correspond to the yellow area in the slice.

During progressive syntectonic deformation, the sides of the pluton experience strain magnitude patterns different from the ones at the ends of the pluton. Strain magnitudes are higher at the sides than at the ends. At the sides, pluton-related and tectonic-related displacement vectors are at low angles and converging to each other, which favors constructive displacement vector interactions. Conversely, at the ends of the pluton, pluton-related and tectonic-related displacement vectors are at high angles to each other, which favors destructive displacement vector interactions. Consequently, regional- and pluton-related strain fields partially cancel each other out, slowing down total strain rates. As a result, total strain intensities at the ends of the pluton are lower than on the sides of the pluton throughout deformation. In addition, during progressive deformation the volume of the low-strain zone decreases. However, symmetry, shape and orientation relative to the pluton of the low-strain zone remain constant.

During progressive deformation, the relative rates of pluton expansion with respect to rates of tectonic deformation have subtle effects on pluton shape, strain magnitude patterns and strain magnitude paths. Higher expansion rates with respect to tectonic deformation rates: (1) increase the sphericity of the pluton; (2) increase strain magnitudes at the sides of the pluton; (3) delay formation of low-strain zones; and (4) favor large

(See opposite page)
Fig. 1. Strain and structural patterns around pluton that expands in a uniaxial shortening tectonic environment. Arrows show direction of maximum shortening. (a)–(d) Two-dimensional strain and structural patterns. Four patterns analyzed simultaneously constrain the direction of maximum shortening and pluton expansion kinematics (see text). (a) Left: undeformed simulation grid. Right: strain magnitude. Dark blue areas represent low strain magnitudes. (b) Foliation. Note foliation triple point at the ends of the pluton; (c) Strain ellipsoid shape. Colors represent values of Lode's parameter. 'Blue' represents constriction and 'pink' represents flattening. (d) Stretching lineations. The *XY* coordinate plane is parallel to the page in Figs. (a), (b) and (c). Conversely, this plane is approximately horizontal in (d), which helps clarify the orientation of lineations for the case where uniaxial shortening is horizontal. In this case, vertical lineations are widespread, unlikely in the non-coaxial case (Guglielmo 1993b) where lineations are restricted to regions of maximum constriction. Patterns (b)–(d) are cross-sections through the center of three-dimensional models in Figs. (i), (l) and (o). (e)–(h) Same patterns as (a)–(d), respectively, however at a more advanced stage of deformation. (e) Strain intensities increase at the sides of the pluton and strain shadows form at the ends of the pluton. Foliation triple points (f) and constrictional regions (g) move towards the pluton. Stretching lineation patterns (h) remained unchanged with progressive deformation. Triple point displacement (arrow in I) smaller than tectonic displacement (arrow in II) suggests that constrictional point migration rates are slower than tectonic displacement rates. Large changes in strain magnitude and shape may occur without changes in foliation deflection (e.g. region III). Pattern e is a cross-section through the center of pluton in (m). (i)–(k) Three-dimensional Lode's parameter patterns. (i) The green ball in the center of the picture represents the pluton (I). A green ring-shaped surface (II) connects points of plane strain, and, therefore, separates regions of constriction within the ring from regions of flattening on the sides of the pluton (top and bottom of i). In regions of flattening, foliations are expected to be better developed than lineations around natural plutons, whereas in regions of constriction stretching lineations would be more conspicuous than foliations. Pink surface (III) envelops the highest constrictional strains and, therefore, is expected to contain the best developed mineral stretching lineations in the region. Surface II corresponds to the boundary between the green and yellow areas in (c), whereas surface III corresponds to the boundary between the blue and green areas. (j) Rotated version of (i). (k) Increasing pluton expansion rates with respect to tectonic rates displaces constrictional rings away from the pluton (cf. j & k). (l) Three-dimensional patterns of foliations. Pink surfaces show pluton and constrictional ring as (i). Blue squares represent orientations and distribution of foliation planes. Foliation is parallel to the pluton next to the pluton (I), perpendicular to the direction of regional shortening far from the pluton (II), and forms triple points within the constrictional ring (III). Real-time 'fly-by' through, and rotation of this three-dimensional model on the computer screen helps visualization of foliation trends drawn in Fig. 3(b). (m) & (n) Three-dimensional strain magnitude patterns. Green elongated ellipsoid in the center (I) represents pluton. (m) A continuous strain shadow ring forms at the ends of the pluton. (n) Lens-shaped zones of high strains form on the sides of the pluton. Cross-sections subparallel to the paper and through the center of these three-dimensional plutons produces the two-dimensional slice shown in (e). (o) Three-dimensional patterns of mineral stretching lineations. Pink surfaces show pluton and constrictional ring as in (j). Yellow segments show orientation and distribution of mineral stretching lineations. Main stretching lineation domains are shown in Fig. 3(b).

(See page 242)
Fig. 2. Strain and structural patterns around pluton that expands in a uniaxial extensional tectonic environment. Arrows show direction of maximum extension. (a)–(d) Two-dimensional strain and structural patterns. Colors have same meaning as in Fig. 1. (a) Strain magnitude, (b) foliation patterns and (c) strain ellipsoid shape. Notice two isotropic points at the ends of the pluton (I). (d) Horizontal stretching lineations form a 'lineation triple point'. (e)–(h) Same patterns as (a)–(d), respectively, however at a more advanced stage of deformation. (e) Strain intensities increase at the sides of the pluton and strain shadows form at the ends of the pluton as in the case of uniaxial shortening. However, in three dimensions these patterns are distinct (see j). Foliation triple points (f) and isotropic points (g) and lineation triple points (h) move, at slow rates, towards the pluton. Patterns (e), (f), (g) and (h) are cross-sections through the center of pluton in (j), (k), (i) and (m), respectively. (i) Strain shape patterns. The blue ellipsoid in the center of the picture (I) represents the pluton. A pink surface is the locus of points of plane strain. This surface separates regions of flattening closer to the pluton from regions of constriction farther away from the pluton. Blue surface (III) is a locus of high constrictional strains (Lode's parameter equals to -0.5). Surface III corresponds, approximately to the boundary between the dark blue and light blue in (g), whereas the pink surface corresponds to the boundary between yellow and green areas. These patterns contrast with patterns formed during uniaxial shortening (Figs. 1i, j & k). (j) Strain magnitude patterns. Pink ellipsoid in the center (I) represents pluton. Pink zones of high strains form on the sides of the pluton (II), whereas green ellipsoidal low-strain zones form at the ends of the pluton (III). A cross-section sub parallel to the paper and through the center of the pluton and low-strain zones produces the two-dimensional slice shown in Fig. 1(e). Surface II corresponds to the boundary between green and blue areas in the slice, therefore, strains in high-strain regions range between 1.0 and 2.5. Conversely, surface III corresponds approximately to the dark blue low-strain zones, where, strain magnitude values are lower than 0.5. These patterns contrast with patterns formed during uniaxial shortening (Figs. 1m & n). (k) & (l) Foliation patterns. Pink plane-strain surfaces show constrictional regions (as surface III in Fig. 1i) around pluton. Blue squares represent orientations and distribution of foliation planes. The picture on the left (k) is a rotated version of the model on the right (l). Foliation form concentric patterns about the axis of maximum regional extension. Main foliation domains are simplified in Fig. 3(d). (m) Stretching lineations. Pink high-strain surfaces show constrictional regions (as surface II in j) around pluton. Yellow segments represent orientations and distribution of stretching lineations. Without real-time three-dimensional rotations seen in a computer screen, it is difficult to see whether lineations plunge towards or away from the viewer. Therefore, main lineation domains are simplified in Fig. 3(d). (n) Post-tectonic emplacement. Pluton in the center (I) expanded *after* regional deformation. Notice the subspherical shape of the pluton. Green surfaces (II) are the locus of plane strain. Strain patterns are similar to the ones of syntectonic emplacement (i).

(See page 243)
Fig. 3. (a) The orientations of erosional planes (I–VII) with respect to the direction of maximum regional shortening (arrows) produce strain map patterns shown in Fig. 4. (b) Foliation and stretching lineation form irregular rings around the pluton. Syntectonic uniaxial shortening (arrows) and pluton expansion transformed an initial cube (white dashed lines) into a parallelepiped (white continuous lines). Background photograph is the same as Fig. 1(o), where the doughnut-shaped surface around the pluton separates regions of constriction from regions of flattening. Shaded planes represent average orientations of foliation, whereas thick white dashes represent average orientation of lineations. Foliations form a ring with constant equilateral triangular section at the ends of the pluton (I). Foliations are parallel to the pluton next to the pluton (II) and parallel to regional strains away from the pluton (III). Stretching lineations are concentric about the direction of maximum shortening, parallel to pluton contact, to constrictional ring and to foliation. (c) The orientations of erosional planes (I–VI) with respect to the direction of maximum regional extension (arrows) produce strain map patterns shown in Fig. 5. (d) Foliation and stretching lineation domains around pluton that expanded during uniaxial regional extension and pluton expansion. Syntectonic deformation transformed an initial cube (white dashed lines) into a parallelepiped (white continuous lines). Background photograph is the same as Fig. 2(j), where the ellipsoids at the ends of the pluton represent low-strain zones. Shaded planes represent average orientations of foliation, whereas thick white dashes represent average orientation of lineations. Foliations are parallel to the pluton next to the pluton (I and III) and form a cone at each end of the pluton (II). The base of these cones (III) is perpendicular to the direction of maximum extension (arrows). Stretching lineations are parallel to the pluton contact next to the pluton (I and III), parallel to regional strains away from the pluton (IV), and form a cone at each end of the pluton (II).

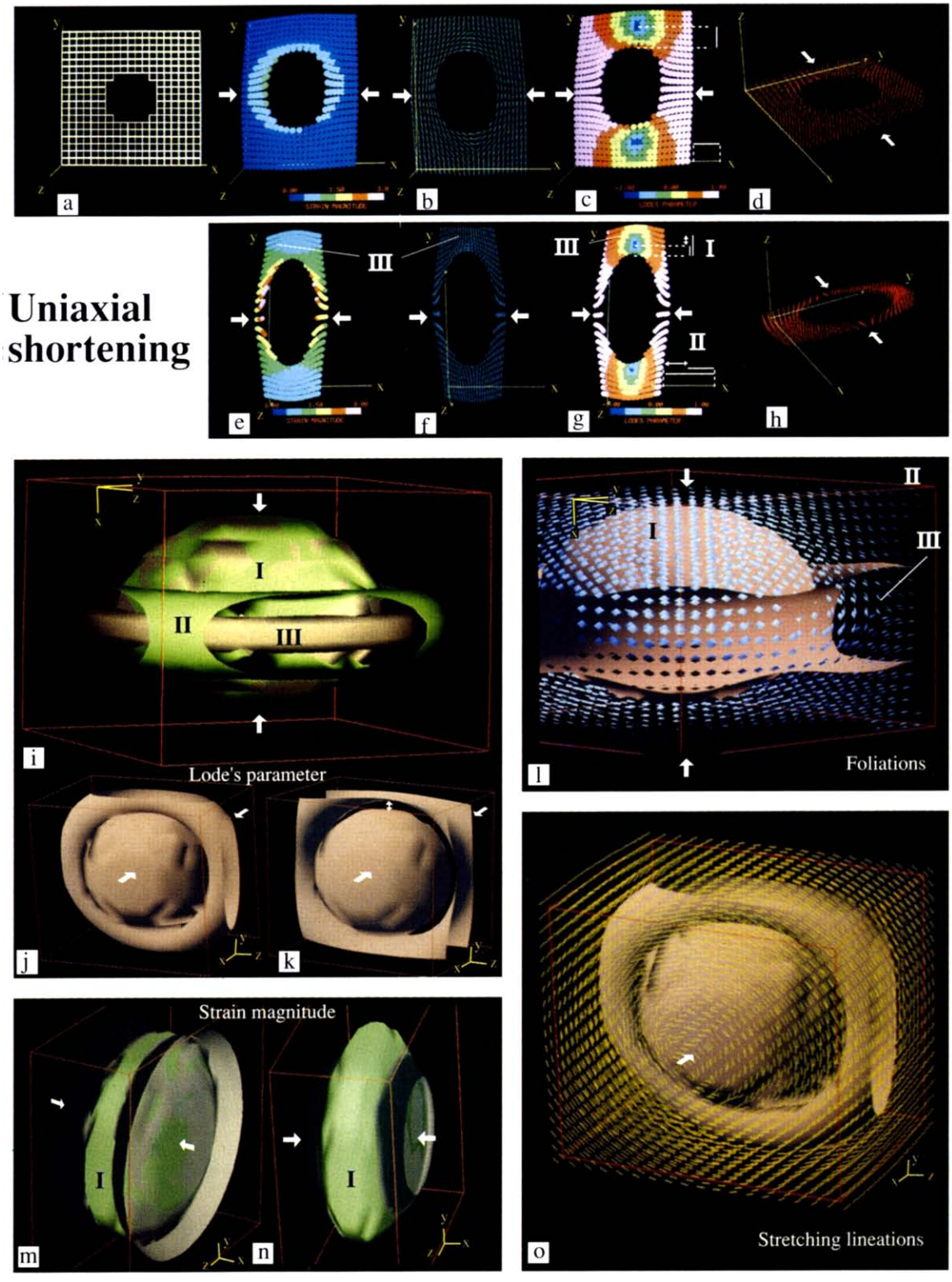
Uniaxial shortening
a
b
c
d
e
f
g
h
III
III
I
II
i
I
II
III
Lode's parameter
j
k
l
II
I
III
Foliations
Strain magnitude
I
I
m
n
o
Stretching lineations

Fig. 1.

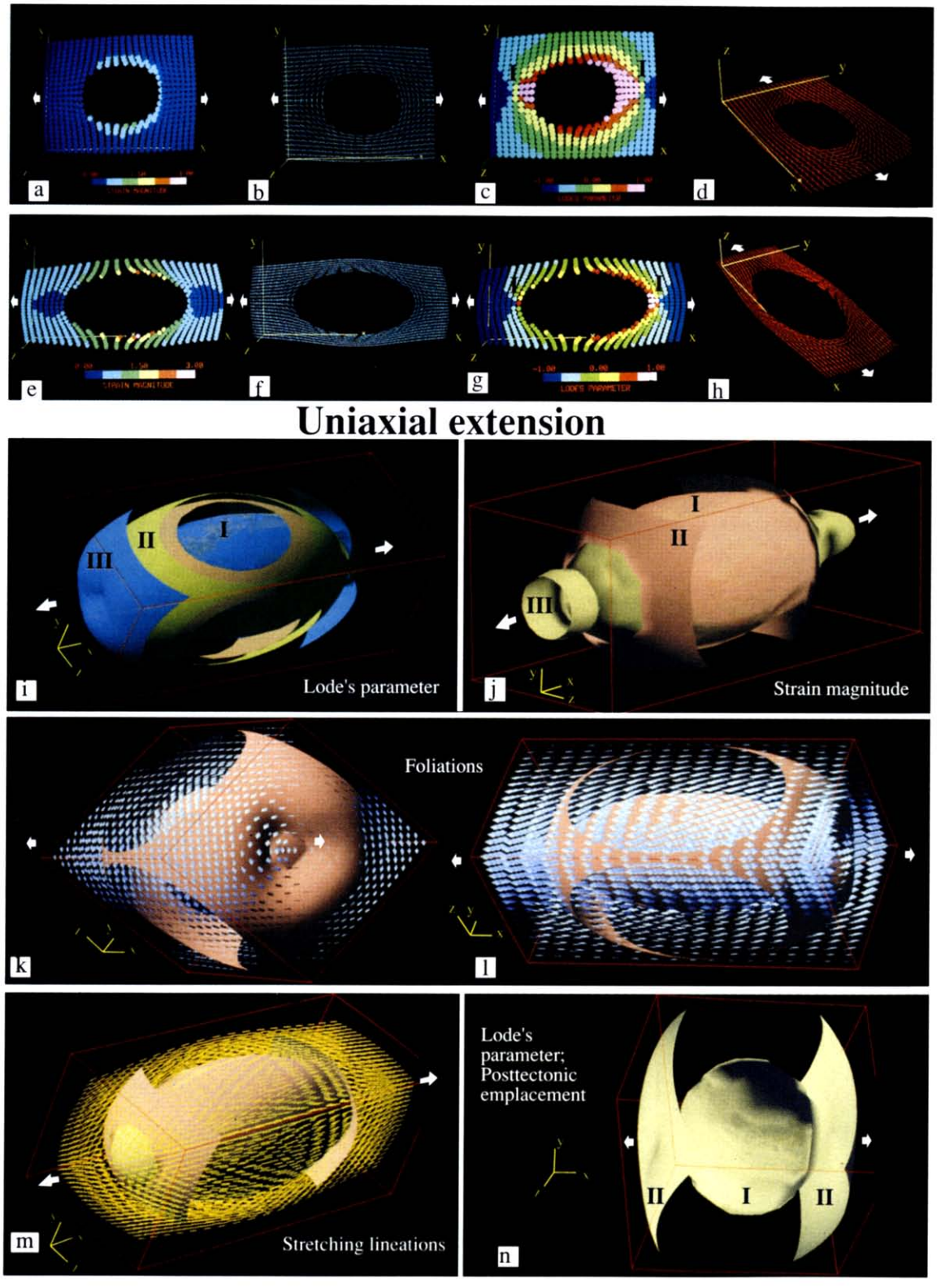
a
b
c
d
e
f
g
h
Uniaxial extension
III
II
I
i
Lode's parameter
I
II
III
j
Strain magnitude
Foliations
k
l
m
Stretching lineations
Lode's
parameter;
Posttectonic
emplacement
II
I
II
n

Fig. 2.

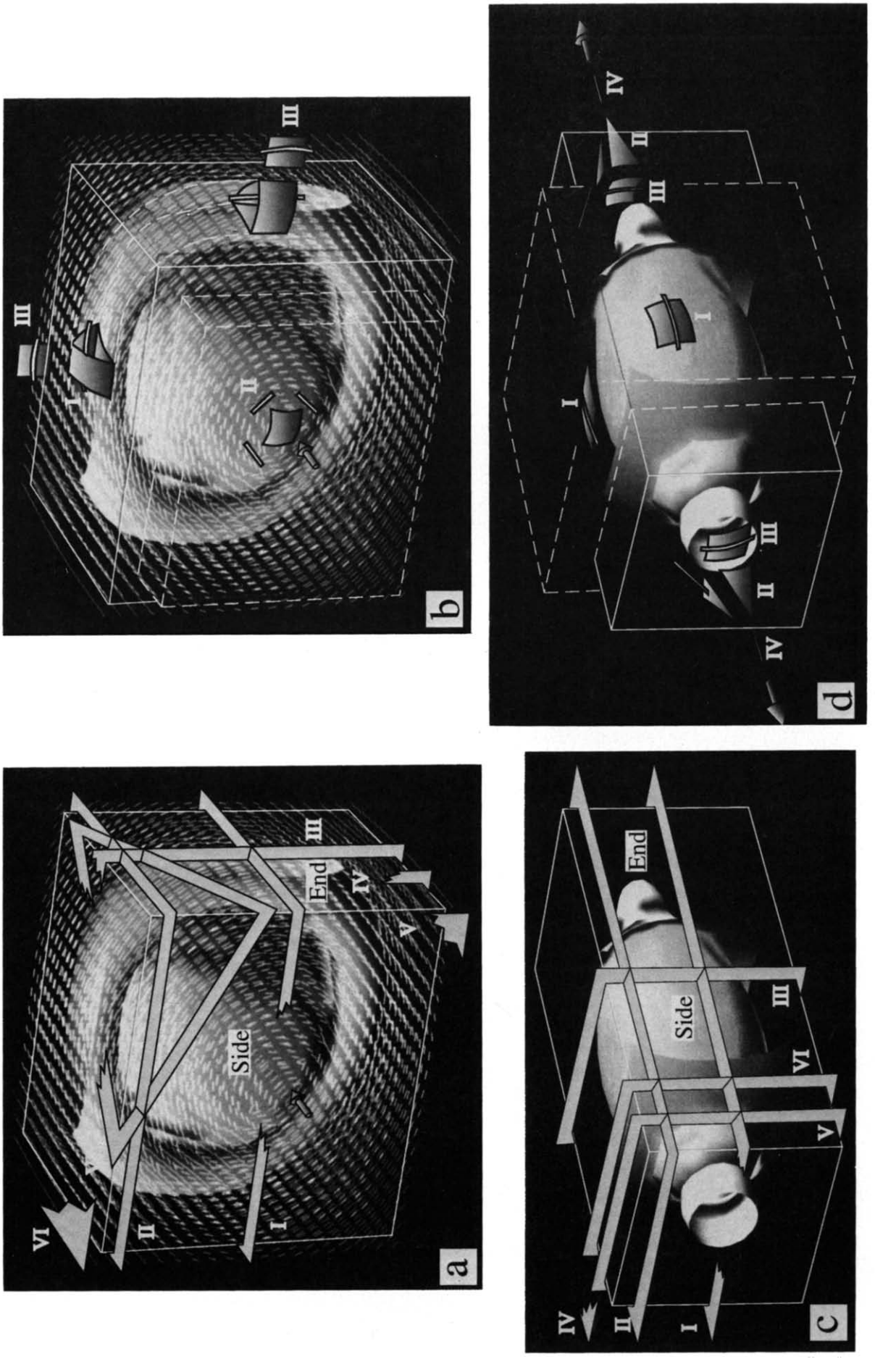
a
Side
End
I
II
III
IV
V
VI
b
I
II
III
c
Side
End
I
II
III
IV
V
VI
d
I
II
III
IV

Fig. 3.

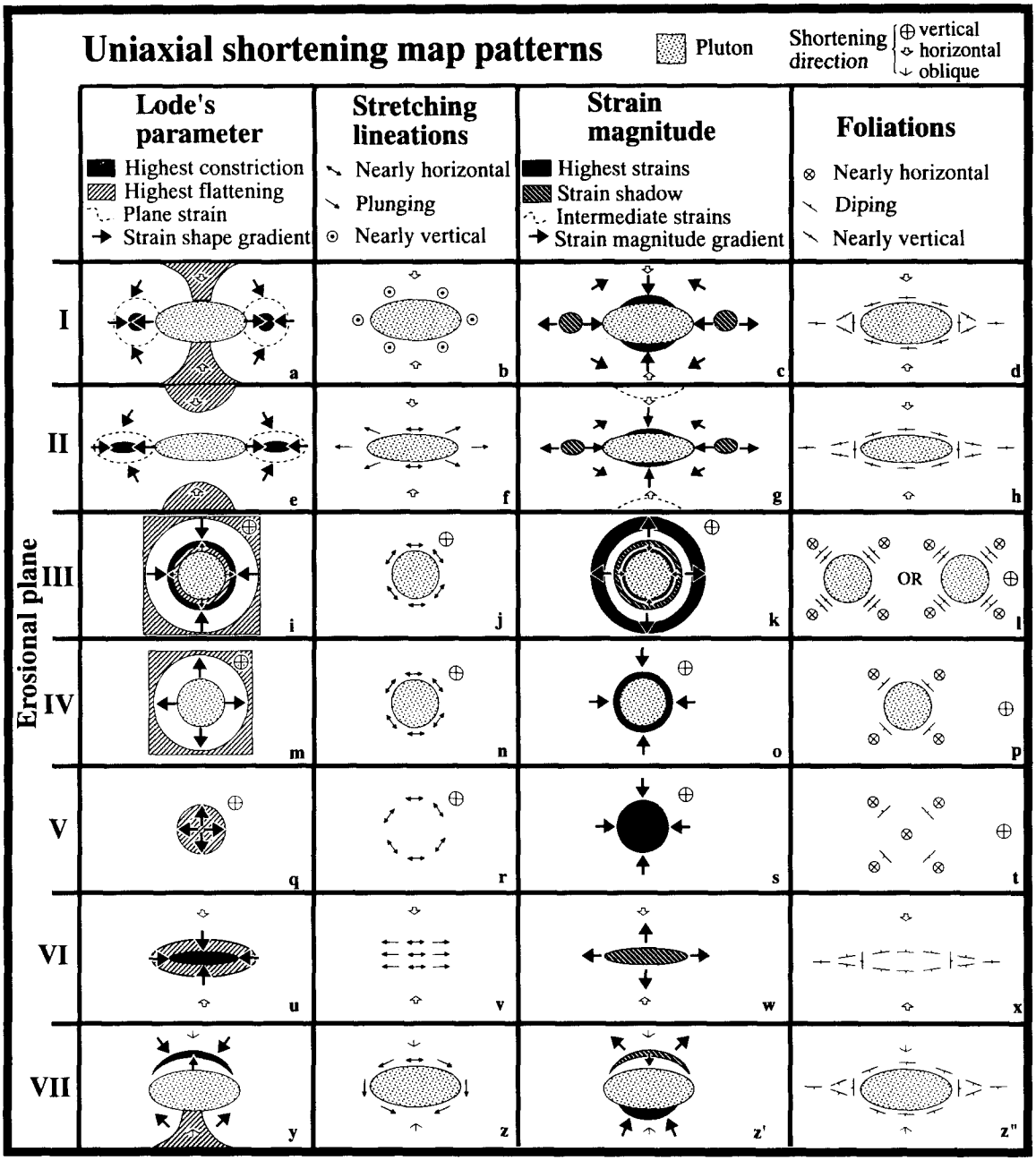

Fig. 4. Various orientations of erosional planes with respect to regional shortening produce distinct strain and structural map patterns. Patterns (I)–(VII) were produced, respectively, by planes (I)–(VII) from Fig. 3(a). Patterns (V), (VI) and (VII) are expected above unexposed plutons. See text for explanation.

low-strain zones. Conversely, higher tectonic deformation rates with respect to expansion rates make the pluton more elongated and favor well-defined, small, low-strain zones early in the deformation history.

Extension. During pluton expansion in a uniaxial extensional tectonic environment, low-strain zones have approximately the shape of two ellipsoids at the ends of the pluton. The major axis of each ellipsoid a_1 (where $a_1 > a_2 = a_3$) is parallel to the major axis of the pluton. Conversely, regions of high strains envelop the pluton with the same three-dimensional geometry of an olive that envelops its seed (Fig. 2j). Strain magnitude absolute values are shown in a two-dimensional slice (Fig. 2e) through the three-dimensional pluton and through the center of both low-strain zones (Fig. 2j). Within the low-strain zone ellipsoids (Fig. 2j), strain magnitudes are lower than 0.5, and correspond approximately to the dark blue area in the two-dimensional slice (Fig. 2e). On the other hand, within the high strain regions (Fig. 2j), strain magnitudes are higher than 1.0, and correspond to the light blue, green and yellow areas in the slice.

During progressive syntectonic deformation, strain magnitude patterns and paths at the sides of the pluton are different from the ones at the ends of the pluton. At the sides of the pluton, pluton-related and tectonic-related displacement vectors are at high angles. Consequently, regional and pluton-related strain fields add up producing faster total strain rates, which, in turn, produce high total strains at any time during progressive

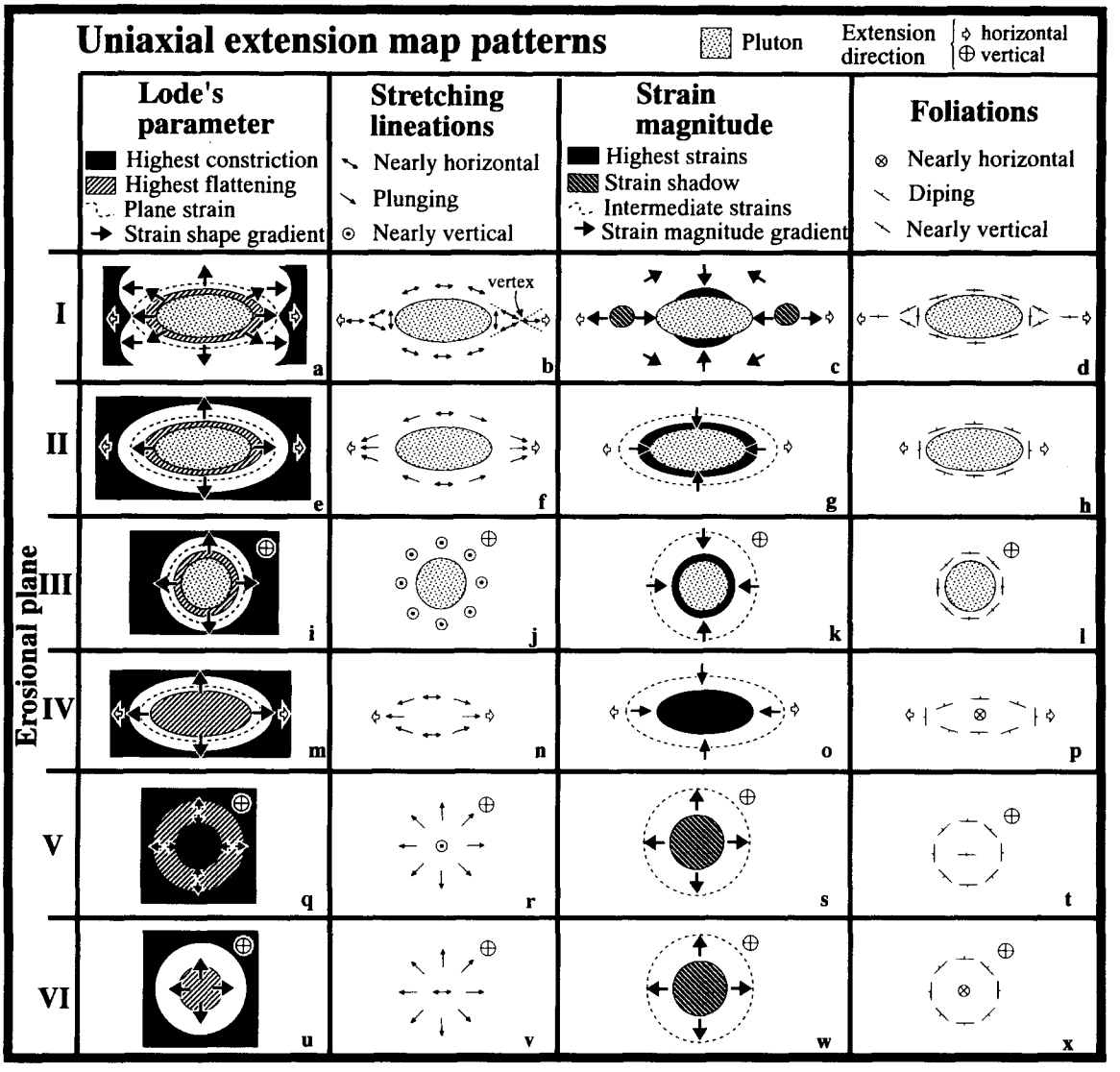

Fig. 5. Various orientations of erosional planes with respect to regional extension produce distinct strain and structural map patterns. Patterns (I)–(VI) were produced, respectively, by planes (I)–(VI) from Fig. 3(c). Patterns (IV), (V) and (VI) are expected above unexposed plutons. See text for explanation.

deformation. Conversely, at the ends of the pluton, pluton-related and tectonic-related displacement vectors are at low angles and displace elements in the country rock approximately towards the same direction. This concordant interaction between strain fields causes rigid-body translation but little internal deformation and, as a result, slow down total strain rates. Consequently, total strain intensities at the ends of the pluton are lower than on the sides of the pluton throughout deformation.

During progressive deformation, higher expansion rates relative to tectonic deformation rates: (1) increase the sphericity of the pluton; (2) rapidly increase strain magnitudes at the sides of the pluton; (3) delay formation of low-strain zones; and (4) favor large low-strain zones. Conversely, higher tectonic deformation rates relative to expansion rates: (1) make the pluton more elongated; (2) produce slow increases in strain magnitudes at the sides of the pluton; and (3) enhance the formation of well-defined, small, low-strain zones early in the deformation history.

Foliation and lineation patterns

Foliation and stretching lineations are worth modeling because the orientation and intensity of these structures in the field provide quick, qualitative information about the orientation, shape and magnitude of the strain ellipsoid.

Although fabrics in natural rocks may form parallel to the last incremental strain ellipsoid and overprint earlier fabrics, this simulation assumes that rocks undergo ideal re-equilibration with the incremental strain ellipsoid throughout the deformation history. Therefore, orientation and intensity of fabrics are defined by the geometry of the total strain ellipsoid. That is, foliation forms parallel to XY plane of the ellipsoid, whereas stretching lineations form parallel to the to X axis of the ellipsoid.

The intensity and type of structures depend on many variables such as rock type, amount of platy and linear minerals, degree of recrystallization and dissolution, etc. However, these structures also depend on the magnitude and shape of the total strain ellipsoid. Therefore,

although it is difficult to specify at which *absolute* values of strain magnitude and shape structures would become noticeable in the field, it is safe to say that well-developed foliation is favored by high-magnitude flattening strains, whereas conspicuous stretching lineations are favored by high-magnitude constrictional strains.

Foliation patterns

Shortening. During pluton expansion in a uniaxial shortening environment, foliation forms a three-dimensional symmetrical ring, which passes around the ends of the pluton and is located within the three-dimensional region of constriction (Figs. 1b & l and 3bI). Conversely, on the side of the pluton, foliation is parallel to the pluton contact next to the pluton (Fig. 3bII), and is parallel to the regional shortening direction away from the pluton (Fig. 3bIII).

The evolution of the foliation ring during progressive syntectonic deformation is similar to the evolution of constrictional rings. The foliation ring migrates, and rates of migration are much slower than the rates of tectonic deformation or rates of pluton expansion. Relative rates of pluton expansion with respect to tectonic deformation affect the position of the foliation ring. During progressive deformation, higher expansion rates relative to tectonic deformation rates displace the ring away from the pluton. Conversely, higher tectonic deformation rates relative to expansion rates bring the ring closer to the pluton.

Extension. During pluton expansion in a uniaxial extensional environment, foliation is parallel to the pluton contact on the sides of the pluton (Figs. 2k & l and 3dI). However, at each end of the pluton foliation planes form cones (Fig. 3dII). The position and orientation of these cones are geometrically tied to other strain patterns and to the shape of the pluton: the position of each cone approximately coincides with the strain shape isotropic point (cf. Figs. 2f & g) and with the position of the low-strain zone (Fig. 2e). In addition, the base of each cone (Fig. 3dIII) is parallel to the contact between the pluton and the wall rock near the cone, so that both cones point away from the pluton.

During progressive deformation, the relative rates of pluton expansion and tectonic deformation change the position but not the orientation of foliation cones. Higher expansion rates with respect to tectonic deformation rates move foliation cones away from the pluton. Conversely, higher tectonic rates with respect to expansion rates bring foliation cones closer to the pluton. Eventually, at very high tectonic rates, foliation cones may touch the ends of the pluton. As with changes in flattening and constriction regions, changes in the position of foliation cones happen at rates that are much slower than rates of tectonic deformation or pluton expansion.

Lineation patterns

Shortening. During pluton expansion in a uniaxial shortening environment, the sides and ends of the pluton show lineations that are parallel to the constrictional ring, and concentrically oriented around the axis of maximum regional shortening (Figs. 1o and 3bI, bII & 3bIII). This pattern of mineral stretching lineations remains constant during progressive coaxial syntectonic deformation. Furthermore, not even changes in relative rates of pluton expansion with respect to tectonic deformation affect this pattern.

Extension. During pluton expansion in an uniaxial extensional environment, stretching lineations are parallel to the elongation of the pluton on the sides of the pluton and parallel to the direction of maximum regional extension away from the pluton (Fig. 3dIV). However, at each end of the pluton, stretching lineations are arranged following the three-dimensional shape of a cone (Figs. 2m and 3dII). As in the case of foliation cones, the position and orientation of lineation cones are geometrically tied to other strain patterns and to the shape of the pluton: the position of each lineation cone approximately coincides with the strain shape isotropic point, with the low-strain zone, and with the foliation cone. In addition, the base of each cone (Fig. 3dIII) is parallel to the contact between the pluton and the wall rock near the cone, so that both cones point away from the pluton.

The effects of progressive deformation on the geometry of stretching lineation cones are analogous to the effects of progressive deformation on foliation cones. During progressive deformation, the relative rates of pluton expansion with respect to tectonic deformation change the position, but not orientation, of lineation cones. Higher expansion rates with respect to tectonic deformation rates move lineation cones away from the pluton. Conversely, higher tectonic rates relative to expansion rates bring lineation cones closer to the pluton. Eventually, at very high tectonic rates, lineation cones may touch the ends of the pluton. As with changes in foliation cones, changes in the position of lineation cones happen at rates that are much slower than rates of tectonic deformation or pluton expansion.

Pre- and post-tectonic plutons

In this simulation, during coaxial deformation, plutons that expand after deformation tend to be more equidimensional than syntectonic plutons. Conversely, plutons that expand before deformation tend to be more elongated than syntectonic counterparts. However, strain patterns resulting from pre- and post-tectonic pluton expansion are analogous to patterns produced during syntectonic expansion: during uniaxial shortening, higher total tectonic strains favor a pattern of well-defined low-strain zones, thin constrictional rings, constrictional, foliation and lineation rings closer to the pluton. Conversely, higher total expansion-related

strains favor a pattern of high strains uniformly distributed around the pluton, as well as fat constrictional rings, constrictional, foliation and lineation rings away from the pluton. Similarly, during uniaxial extension, higher total tectonic strains favor a pattern of well-defined low-strain zones, smaller flattening regions, as well as isotropic points, foliation cones and lineation cones closer to the pluton. Conversely, higher total expansion-related strains favor a pattern of high strains on the sides of the pluton, large flattening regions, as well as isotropic points, foliation cones and lineation cones distant from the pluton.

FIELD IMPLICATIONS

This simulation illustrates three-dimensional patterns of strain shape and magnitude, as well as the orientation of foliation and lineations, formed around a pluton that expands in a coaxial, ductile, tectonic regime. In addition, this simulation provides information about the following questions. What are the location and orientation of maximum gradients of strain shape and magnitude, and where do *L* tectonites predominate over *S* tectonites in strain aureoles? Can ductile strains account for all the room necessary for pluton emplacement? What is the origin of curved and truncated inclusion trails within porphyroblasts? How can we use strain and structural patterns to establish the orientation of regional kinematic schemes in three dimensions?

L–S *tectonites*

Three-dimensional models produced by pluton expansion in a coaxial tectonic environment have relatively few and simple end-member geometries (three-dimensional pictures in Figs. 1 and 2). However, two-dimensional cuts trough these models suggest that map patterns expected can be remarkably diverse (Figs. 4 and 5).

These map patterns suggest (1) that *L* tectonites may predominate over *S* tectonites or vice versa, and (2) the position and orientation of these tectonites. For example, consider a particular erosional plane in Fig. 4 (plane I). High flattening strains on the sides of the pluton (Fig. 4a) are likely to produce *S* tectonites. These rocks would have poorly developed, vertical stretching lineations (Fig. 4b) and extremely well-developed, vertical foliations that form two triple points (Fig. 4d). Conversely, regions of high constriction at the ends of the pluton (Fig. 4a) will generate *L* tectonites, which have well-developed, vertical, mineral stretching lineations (Fig. 4b) and horizontal, poorly developed or absent foliations (Fig. 4d). This region of *L* tectonites is limited within foliation triple points (Fig. 4d) and therefore is well defined and easy to locate in the field.

The analysis described for plane I of Fig. 4 may be adapted to describe the remaining map patterns shown in Figs. 4 and 5.

Strain gradients

Large variations in strain magnitudes and shapes are easier to measure in the field, and traverses along strong strain gradients are kinematically more informative, than randomly chosen traverses. It is commonly difficult to identify which traverses near plutons will yield the most information. This simulation suggests locations for traverses that show maximum strain gradients.

Three-dimensional models and map patterns suggest that the *absence* of structures can indirectly identify low-strain zones and consequently suggest the orientation of strain gradients. This fact reinforces that absence of structures in the field is data worth recording. However, direct strain measurements provide more accurate strain gradients. Black arrows in two-dimensional erosional cuts (Figs. 4 and 5) suggest maximum gradients of strain shape and magnitude. Traverses along lines indicated by these arrows would contain outcrops where variations of strain are maximized. Therefore, these arrows suggest locations for the most informative strain and structural traverses around natural plutons.

In addition, three-dimensional modeling suggests how pluton expansion can produce complex strain shape gradients. Both pluton expansion and regional uniaxial shortening, when acting separately, produce relatively simple three-dimensional flattening fields. However, interactions between these two flattening fields generate constrictional strains locally and, consequently, produce steeper and more complex strain shape gradients regionally. Local constrictional strains appear where pluton-related and tectonic-related displacement vectors interact destructively. Therefore, the steepest strain shape gradients form along lines connecting regions of maximum constructive to maximum destructive displacement vector interactions. Strain shape gradients are nearly parallel to strain magnitude gradients during pluton expansion and uniaxial shortening (e.g. black arrows in Fig. 4a are approximately parallel to arrows in Fig. 4c). This 'coincidence' happens because constructive vector interactions that produce flattening strains in a regional shortening environment also produce high-strain magnitudes. Similarly, destructive displacement vector interactions that produce high constriction also produce low-strain zones. Therefore, during uniaxial shortening, strain magnitude gradients and strain shape gradients are geometrically interdependent and approximately parallel to each other.

This interdependence is different for the interaction between pluton expansion and uniaxial extension. During uniaxial extension dominant regional strains are ideally constrictional, and pluton-related strains are ideally flattening. Because maximum strain gradients form along lines that connect maximum constriction to maximum flattening, pluton expansion and regional extension interact to produce approximately radial maximum strain *shape* gradients (Fig. 5a). Conversely, regional constrictional strains interact with local flattening strains to produce two low-strain regions at the ends of the pluton, thereby creating complex strain *magnitude*

gradients (Fig. 5c). Therefore, during pluton expansion and regional uniaxial extension, strain shapes and strain magnitudes are interdependent but, unlike the shortening case, maximum strain shape and magnitude gradients are not parallel to each other.

It is noteworthy that two-dimensional strain patterns can be ambiguous, especially if taken individually (cf. Figs. 4c and 5c). This suggests that the four modeled parameters should be analyzed in combination. Fortunately, the three-dimensional modeled structures (three-dimensional pictures in Figs. 1 and 2) have unique but relatively simple symmetry. Consequently, the reader can mentally rotate and slice the models to create additional map patterns to compare with strains in aureoles of natural plutons.

Width of strain aureoles

The width of strain aureoles can be used to estimate impact of pluton-related strains in the country rock and to evaluate mechanisms to account for room necessary for pluton emplacement. Lack of foliation deflection around plutons is commonly used to infer narrow strain aureoles. However, this simulation indicates that: (1) ductile strains may strongly affect country rocks without deflecting foliations; and (2) the region of ductile strains around the pluton may be much larger than the region affected by foliation deflection. Consequently, measurements of foliation deflections may underestimate aureole widths.

Foliation deflections manifested as triple points are most useful when used to determine a *minimum* width for strain aureoles (Guglielmo 1993b). In addition, foliation and lineation deflections describe changes in only one aspect of the strain ellipsoid: strain orientation. However, strain ellipsoid shape and magnitude may also change in the country rock due to pluton emplacement and contribute to strains in aureoles. Depending on the orientation of regional vs local displacement vectors, and on strain gradients, these changes can affect country rocks far from the pluton (cf. Figs. 1e & g). Simultaneously, lineation and foliation orientation in these regions can remain constant, and mistakenly suggest narrow strain aureoles.

This simulation also suggests that, besides ductile flow, rigid-body translation is an important and commonly overlooked mechanism to account for room for pluton emplacement. At any given point around the pluton, ductile flow will predominate over rigid-body translation if local and regional displacement vectors have the same trend but point to opposite directions (e.g. in sides of pluton in Figs. 1e & n). Conversely, rigid-body translation will increase relative to ductile flow if these displacement vectors have the same trend and point in same direction (e.g. within low-strain zones in Figs. 1e & m). Therefore, rigid-body translation clearly affects strain patterns around the pluton. However, unlike ductile flow, rigid-body translation does not increase strain magnitudes. Consequently, although rigid-body translation can be an important mechanism to make room for pluton emplacement, this mechanism can be overlooked. These conclusions are true for non-coaxial (Guglielmo 1993b) and coaxial deformation, as well as for pre-, syn- and post-tectonic pluton expansion.

Inclusion trails within porphyroblasts

Cross-cutting relationships between inclusion trails within porphyroblasts (*Si*) and external foliation in strain aureoles (*Se*) are commonly used to determine relative timing of pluton emplacement and regional deformation. However, porphyroblast growth and consequent formation of *Si* may stop at any time during syntectonic emplacement, while foliation ring or cone migrations may continuously change the orientation of *Se*. The result can be highly discordant *Si–Se* relationships similar to the ones associated with pre-tectonic porphyroblasts. As a consequence, syntectonic expanding plutons can produce either 'pre- or syntectonic' contact metamorphic porphyroblasts. In addition, pre-, syn- and post-tectonic pluton expansion may produce similar foliation patterns in the country rock (see *Results of pre- and post-tectonic case* section) and consequently generate similar *Se–Si* relationships. Therefore, timing relationships between pluton emplacement and tectonic deformation derived from *Si–Se* cross-cutting relationships in contact aureoles may be ambiguous.

Inclusion trails within porphyroblasts commonly show complex patterns and high-angle truncations, which have been explained as resulting from overprinting of near-orthogonal foliations upon non-rotating porphyroblasts. It has been suggested (Bell & Johnson 1989, Hayward 1990, Bell & Hayward 1991, Bell *et al.* 1992) that these near-orthogonal foliations could be created by regional horizonal shortening that produces vertical foliations, followed by regional gravitational collapse that produces horizontal foliations. This simulation suggests an additional mechanism to explain complex sequences of high-angle overprinting of foliations and the evolution of inclusion trails within porphyroblasts. Truncated and curved inclusion trails may form as a result of ordinary geological process involving migration of foliation rings (or cones) at the ends of plutons. For example, consider the following scenario: a foliation ring or cone is displaced away from the pluton by a new pulse of magma or by decreasing tectonic deformation rates (Fig. 6). In map view, ring and cones are represented by triangles (e.g. foliation triple point in Fig. 6) whose base is parallel to pluton contact and sides form high angles with pluton contact. Foliation around a porphyroblast in the path of a ring (Fig. 6c) rotates, relative to the porphyroblast, as the ring passes by. If the ring migrates away from the pluton, foliation that originally formed high angles with the pluton contact (Fig. 6c, stage 1) will now form low angles (Fig. 6c, stage 2). Simultaneously, porphyroblast growth due to progressive contact metamorphism could record this change of foliation orientation as inclusion trails. Incomplete re-equilibration between total strain ellipsoid and foliation development may produce crenulated foliations in the

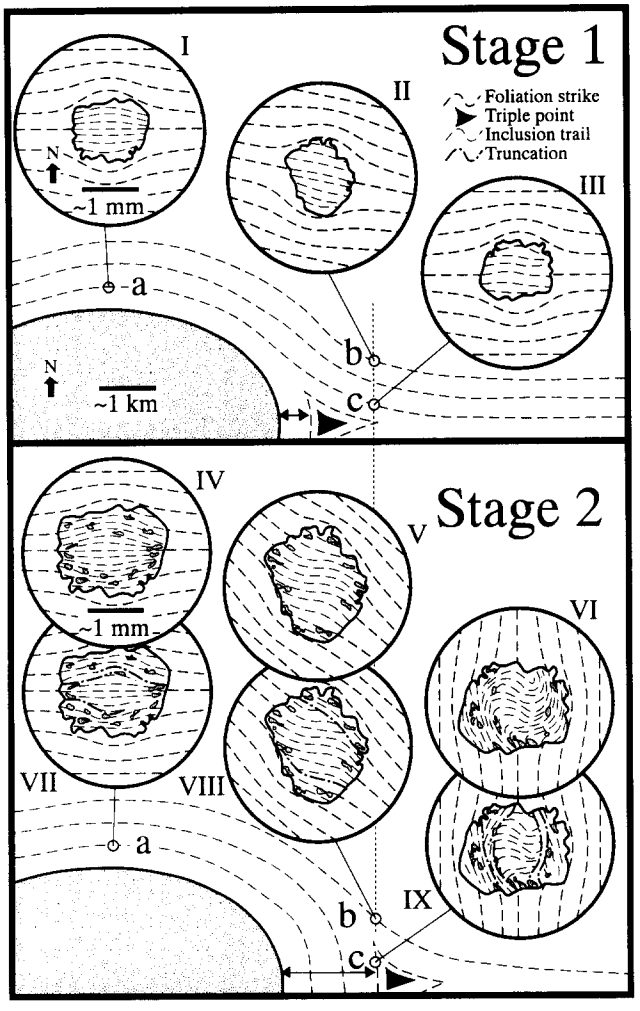

Fig. 6. Foliation ring migration (arrow) explains complex patterns of inclusion trails within porphyroblasts (IV–IX) around a pluton. From stage 1 to stage 2 foliation triple points gradually migrate away from the pluton. Growth rates are moderate, constant, and the same for all porphyroblasts. On the sides of the pluton (a) orientation of foliation and, consequently, of inclusion trails remains *constant* during progressive deformation (I and IV). Truncations may form sporadically if there are abrupt changes in tectonic deformation rates, or if sudden pulses of magma cause abrupt expansion or rising of the pluton. However, truncations would form subparallel to inclusion trails (VII). Between sides and ends of the pluton (b) orientation of foliation changes *gradually* during progressive deformation. Therefore, porphyroblast growth records curved inclusion trails (V). As within porphyroblasts at the sides of the pluton, truncations may form sporadically within porphyroblasts between sides and ends of the pluton. However, angles between two subsequent truncations or between truncations and inclusion trails are low to moderately high (VIII). At the ends of the pluton (c) porphyroblasts are in the path of foliation ring migration. Therefore, foliation orientation changes *abruptly* with progressive deformation (cf. III and VI). Consequently, inclusion trails are highly sigmoidal (VI) and high-angle truncations, are common (IX).

matrix and consequently, in the rim of the porphyroblast. However, in general, the center of the porphyroblast records the foliation orientation at stage 1, whereas the rim of the porphyroblast records foliation orientation at stage 2 (cf. Figs. 6III & VI).

Ring migrations might explain the coexistence and relative abundance of curved vs truncated trails. Truncations are favored by non-uniform porphyroblast growth rates, abrupt tectonic events, or sudden pluton expansion and rising. In addition, this simulation shows that *constant* orientation and style of pluton-related and tectonic-related strain fields may cause ring migrations and complex microstructures within porphyroblasts. Small ring displacements cause high foliation rotation rates around porphyroblasts that are in the direct path of the ring (cf. Figs. 6III & VI). These high rotations rates favor high-angle truncations (e.g. Fig. 6IX). Conversely, the same ring displacement and porphyroblast growth rates cause comparatively low foliation rotation rates around porphyroblasts located between the ring and the sides of the pluton (cf. Figs. 6II & V). Consequently, curved trails (e.g. Fig. 6V) are expected to be more common than truncated trails. Finally, foliation rotation rates are almost zero around porphyroblasts in the sides of the pluton (cf. Figs. 6I & IV). Therefore inclusion trails, rare truncations and foliations are expected to be approximately parallel to each other.

Ring migration might also explain inclusion trails that show *multiple* truncations within porphyroblasts. As tectonic deformation rates increase relative to pluton expansion rates, foliation rings will move back closer to the pluton, reorienting foliation and inclusion trails within porphyroblasts. This alternation between periods where rings move away from the pluton and periods where rings move towards the pluton can happen indefinitely because new pulses of magma and variations in tectonic strain rates are common. Consequently, a ring may pass over an individual porphyroblast many times producing increasingly complex, curved and truncated, inclusion trails.

Furthermore, curved inclusion trails are commonly assumed to be the result of porphyroblast rotation and, therefore are used to infer sense of shear (Zwart 1962, Rosenfeld 1968, Schoneveld 1977, Vissers 1989). However, curved trails are not, *necessarily*, the result of porphyroblast rotation (Fyson 1975, 1980, Bell 1986, Vernon 1989). Ring migration corroborates this hypothesis by providing a mechanism for formation of curved inclusion trails that does not *require* rotation of the porphyroblast.

In addition, this ring migration mechanism is applicable to many emplacement scenarios. Foliation rings may: (1) appear even if no pluton is visible in the present erosional plane; (2) form around expanding or non-expanding plutons as well as during non-coaxial and coaxial regional deformation; and (3) tend to persist over pre-, syn- and post-tectonic pluton emplacement (Guglielmo 1993b).

Regional kinematic schemes

The orientation and style of regional-scale kinematic schemes are fundamental to reconstructions of orogenic belt history. However, kinematic schemes at regional scale are usually difficult to determine accurately because: (1) pluton-related strains may distort structural trends used to infer the orientation of regional strains; and (2) most kinematic indicators work best at the thin-section or outcrop scale. The four modeled strain ellipsoid patterns, used in combination, are distinct enough

to aid in characterizing type and orientation of the kinematic scheme at a regional scale.

Coaxial and non-coaxial regional kinematic schemes produce distinct strain patterns. Non-coaxial deformation (Guglielmo 1993b) and uniaxial extension (e.g. Fig. 2j) produce two low-strain zones at the ends of the pluton. Conversely, uniaxial shortening forms a continuous low-strain zone ring around the pluton (Fig. 1m). In addition, non-coaxial deformation forms irregular constrictional, lineation and foliation rings parallel to the regional shear direction. Conversely, coaxial deformation forms regular, symmetrical patterns (e.g. Figs. 1o and 2i). Specifically, uniaxial shortening forms constrictional rings perpendicular to the maximum shortening direction, whereas uniaxial extension forms apple-shaped flattening regions aligned parallel to the direction of maximum extension. These patterns are diagnostic of the kinematic schemes that produced them.

The three-dimensional orientation of the direction of maximum regional strain can be derived from strain patterns in aureoles. The direction of maximum *shortening* is perpendicular to the low-strain, lineation, foliation and constrictional rings (e.g. Figs. 1m and 3b). In addition, if regional ductile strain and symmetric radial expansion are thought to be the only causes of wall rock strains and the elongated shape of a given pluton, the minor axis of the pluton may indicate the direction of maximum shortening. Conversely, for uniaxial extension, the direction of maximum *extension* is given by the orientation of the *major* axis of the pluton. In addition, the direction of maximum extension connects two isotropic points (e.g. Figs. 2c & g), and connects the vertices of two symmetrical cleavage or stretching lineation cones (Fig. 3d). In the field, the vertex of each cone is determined by the intersection between two stretching lineations that form the same high angles with the pluton boundary at the end of the pluton (e.g. Fig. 5b). Furthermore, the direction of maximum regional strain may indicate pluton tilt. Specifically, for the uniaxial extension case, the plunge of the direction of maximum regional extension is equal the angle between pluton major axis and the horizontal erosional surface.

In summary, the three-dimensional models suggest that strain patterns around expanding plutons can be useful to identify pluton tilt and three-dimensional orientation or end-member regional kinematic schemes.

CONCLUSIONS

This contribution presents three-dimensional patterns of strain shape and magnitude as well as the orientation of foliation and lineations formed around a pluton that expands in a coaxial, ductile, tectonic regime. Foliation is assumed to form along the XY plane of the total strain ellipsoid and lineations along the X axis of this ellipsoid. Uniaxial shortening produces concentric lineations, symmetrical foliation rings of triangular section, doughnut-shaped constrictional rings and continuous zones of low strain. During uniaxial shortening, higher total tectonic strains favor a pattern of well-defined low-strain zones, thin constrictional rings, as well as constrictional, foliation and lineation rings closer to the pluton. Conversely, higher total expansion-related strains favor a pattern of high strains uniformly distributed around the pluton, fat constrictional rings, as well as constrictional, foliation and lineation rings distant from the pluton.

Uniaxial extension produces two foliation and lineation cones; apple-shaped regions of constrictional strains; and two isolated zones of low strains. During uniaxial extension, higher total tectonic strains favor a pattern of well-defined low-strain zones, smaller flattening regions, as well as isotropic points, foliation cones and lineation cones closer to the pluton. Conversely, higher total expansion-related strains favor a pattern of high strains on the sides of the pluton, large flattening regions, as well as isotropic points, foliation cones, and lineation cones farther from the pluton.

Moreover the simulation shows the origin, location and orientation of: (1) maximum gradients of strain shape and magnitude, which aid in choosing structural traverses in geological maps; and (2) regions where L tectonites predominate over S tectonites, and vice versa.

Furthermore, the simulation provides insights into strain and microstructural observations around natural plutons by showing that: (1) foliation deflections by themselves are insufficient to evaluate width of strain aureoles; (2) rigid-body translation can be an important component to account for room required for pluton emplacement; and (3) strain aureoles around expanding plutons in a ductile crust may be wider than previously thought.

In addition, the simulation shows: (1) how inclusion trails within porphyroblasts may provide misleading timing relationships and sense of shear; and (2) that relatively simple three-dimensional ring or cone migrations can explain complex sigmoidal as well as truncated inclusion trails within porphyroblasts around plutons.

Finally, the modeled patterns and cross-sections show that strain patterns around expanding plutons, when used in conjunction with mesoscopic and microscopic kinematic indicators, can be useful to orient end-member regional kinematic schemes in three-dimensions.

Acknowledgements—This work was supported by National Science Foundation grant number EAR-8904706 and by a UC President's fellowship. I would like to thank S. F. Wojtal, J. M. Dixon and an anonymous reviewer for reading the manuscript.

REFERENCES

Ahren, J. L., Turcotte, D. L. & Oxburgh, E. R. 1980. On the upward migration of an intrusion. *J. Geol.* **89**, 421–432.

Bateman, R. 1985. Aureole deformation by flattening around a diapir during in situ ballooning: The Cannibal Creek granite. *J. Geol.* **93**, 293–310.

Bell, T. H. 1986. Foliation development and shifting patterns of deformation partitioning. *J. metamorph. Geol.* **4**, 421–444.

Bell, T. H., Forde, A. & Hayward, N. 1992. Do smoothly curving spiral-shaped inclusion trails signify porphyroblast rotation? *Geology* **20**, 59–62.

Bell, T. H. & Hayward, N. 1991. Episodic metamorphic reactions during orogenesis: The control of deformation partitioning on reaction sites and duration. *J. metamorph. Geol.* **9**, 619–640.

Bell, T. H. & Johnson, S. E. 1989. Porphyroblast inclusion trails: The key to orogenesis. *J. metamorph. Geol.* **7**, 279–310.

Bergantz, G. W. 1989. Underplating and partial melting: implications for melt generation and extraction. *Science* **245**, 1093–1095.

Berner, H., Ramberg, H. & Stephansson, O. 1972. Diapirism in theory and experiment. *Tectonophysics* **15**, 197–218.

Brun, J.-P., Gapais, D. & Cogne, J. P. 1990. The Flamaville Granite (Northwest France): an unequivocal example of a syntectonically expanding pluton. *Geol. J.* **25**, 271–286.

Brun, J.-P. & Pons, J. 1981. Strain patterns of pluton emplacement in a crust undergoing non-coaxial deformation, Sierra Morena, Southern Spain. *J. Struct. Geol.* **3**, 219–230.

Castro, A. 1986. Structural pattern and ascent model in the Central Extramadura batholith, Hercynian belt, Spain. *J. Struct. Geol.* **8**, 633–645.

Corriveau, L. 1992. Sequential emplacement of magmas in a ballooning potassic alkaline pluton, SW Grenville Province. *Eos* **73**, 282.

Coward, M. P. 1981. Diapirism and gravity tectonics: report of a Tectonic Studies Group conference held at Leeds University, 25–26 March 1980. *J. Struct. Geol.* **3**, 89–95.

Cruden, A. R. 1988. deformation around a rising diapir modeled by creeping flow past a sphere. *Tectonics* **7**, 1091–1101.

Daly, R. A. 1903. The mechanism of igneous intrusions. *Am. J. Sci.* **16**, 107–126.

Daly, R. A. 1933. *Igneous Rocks and the Depths of the Earth*. McGraw-Hill, New York.

Dimroth, E., Mueller, W., Daigneault, R., Brisson, H., Poitras, A. & Rocheleau, M. 1986. Diapirism during regional compression: the structural pattern in the Chibougamau region of the archean Abitibi belt, Québec. *Geol. Rdsch.* **73**, 715–736.

Dixon, J. M. 1975. Finite strain and progressive deformation in models of diapiric structures. *Tectonophysics* **28**, 89–124.

Fyson, W. K. 1975. Fabrics and deformation of Archean metasedimentary rocks, Ross Lake–Gordon Lake area, Slave Province, Northwest Territories. *Can. J. Earth. Sci.* **12**, 756–776.

Fyson, W. K. 1980. Fold fabrics and emplacement of an Archean granitoid pluton, left Lake, Northwest Territories. *Can. J. Earth Sci.* **17**, 325–332.

Goodchild, J. G. 1982. Note on granite junction in the Ross of Mull. *Geol. Mag.* **9**, 447–451.

Guglielmo, G., Jr. 1992. 3-D computer graphics in modeling pluton emplacement. In: *Computer Graphics in Geology* (edited by Pflug, R. & Harbaugh, J. W.). *Lecture Notes in Earth Sciences, Volume* 41. Springer, New York, 171–185.

Guglielmo, G., Jr. 1993a. Magmatic strains and foliation triple points of the Merrimac plutons, northern Sierra Nevada, California. Implications for pluton emplacement and timing of subduction. *J. Struct. Geol.* **15**, 177–189.

Guglielmo, G., Jr. 1993b. Interference between pluton expansion and non-coaxial deformation: three-dimensional computer model and field implications. *J. Struct. Geol.* **15**, 593–608.

Hayward, N. 1990. Determination of early fold axis orientations within multiply deformed rocks using porphyroblasts. *Tectonophysics* **179**, 353–356.

Holder, M. T. 1981. Some aspects of intrusion by ballooning: the Ardara pluton. *J. Struct. Geol.* **3**, 89–95.

Holmes, A. 1965. *Principles of Physical Geology*. Ronald Press, New York.

Huppert, H. O. E. & Sparks, R. S. J. 1988. The generation of granitic magmas by intrusion of basalt into continental crust. *J. Petrol.* **29**, 599–624.

Hutton, D. H. W. 1988. Granite emplacement mechanisms and tectonic controls: inferences from deformation studies. *Trans. R. Soc. Edinb., Earth Sci.* **79**, 245–255.

Jackson, M. P. A. & Talbot, C. J. 1989. Anatomy of mushroom-shaped diapirs. *J. Struct. Geol.* **11**, 211–230.

Koide, H. & Bhattacharji, S. 1975. Formation of fractures around magmatic intrusions and their role in ore localization. *Econ. Geol.* **70**, 781–799.

Ledru, P. & Brun, J. P. 1977. Utilisation des fronts et des trajectories de schistosité dans l'étude des relations entre tectonique et intrusion granitique: example du granite de Flamanville (Manche). *C. r. Acad. Sci., Paris* **285**, 1199–1202.

Lode, W. 1926. Versuche uber den Einfluss der mittleren Hauptspannung auf das fliessen des Matalle Eisen, Kupfer, and Nickel. *Z. Phys.* **36**, 913–939.

Mandal, N. & Chakraborty, C. 1990. Strain fields and foliation trajectories around pre-, syn-, and post-tectonic plutons in coaxially deformed terranes. *Geol. J.* **25**, 19–23.

Marsh, B. D. 1982. On the mechanics of igneous diapirism, stoping and zone melting. *Am. J. Sci.* **282**, 808–855.

Morgan, J. 1980. Deformation due to the distension of cylindrical igneous contacts: a kinematic model. *Tectonophysics* **66**, 167–178.

Morgan, S. S., Law, R. D. & Sylvester, A. G. 1991. Strain-path partitioning during contact metamorphism and emplacement of the Papoose Flat pluton, eastern California. *Geol. Soc. Am. Abs. w. Prog.* **23**, 175.

Paterson, S. R. & Fowler, T. K. 1993. Towards a new paradigm for pluton emplacement studies. *J. Struct. Geol.* **13**, 191–206.

Ramberg, H. 1972. Theoretical models of density stratification and diapirism in the earth's crust. *J. geophys. Res.* **77**, 877–889.

Ramsay, J. G. 1989. Emplacement kinematics of a granite diapir: the Chindamora batholith, Zimbabwe. *J. Struct. Geol.* **11**, 191–209.

Roberts, J. L. 1970. The intrusion of magma into brittle rocks. In: *Mechanics of Igneous Intrusion* (edited by Newall, G. & Rast, N.). Gallery Press, London, 287–338.

Rosenfeld, J. L. 1968. Garnet rotations due to the major Paleozoic deformations in southeast Vermont. In: *Studies of Appalachian Geology: Northern and Maritime* (edited by Zen, E. *et al.*). Interscience, New York, 185–202.

Sanderson, D. J. & Meneilly, A. W. 1981. Analysis of three-dimensional strain modified uniform distributions: andalusite fabrics from a granite aureole. *J. Struct. Geol.* **3**, 109–116.

Schmeling, H., Cruden, A. R. & Marquart, G. 1988. Finite deformation in and around a fluid sphere moving through a viscous medium: implications for diapiric ascent. *Tectonophysics* **149**, 17–34.

Schoneveld, C. 1977. A study of some typical inclusion patterns in strongly paracrystalline rotated garnets. *Tectonophysics* **39**, 453–471.

Schwerdtner, W. M. 1981. Identification of gneiss diapirs (Abstract). p. 90, in Diapirism and gravity tectonics: report of a Tectonic Studies Group conference held at Leeds University, 25–26 March 1980. *J. Struct. Geol.* **3**, 89–95.

Schwerdtner, W. M. & Troeng, B. 1978. Strain distribution within arcuate diapiric ridges of silicone putty. *Tectonophysics* **50**, 13–28.

Seltmann, R. & Bankwitz, P. 1992. Emplacement mechanisms of the Late-Hercynian Tin granites in the Erzgebirge, Germany. *Eos* **73**, 275.

Sylvester, A. G., Oertel, G., Nelson, C. A. & Christie, J. M. 1978. Papoose Flat pluton: a granite blister in the Inyo Mountains, eastern California. *Bull. geol. Soc. Am.* **89**, 1205–1219.

Tobisch, O. T., Saleeby, J. B. & Fiske, R. S. 1986. Structural history of continental volcanic arc rocks, eastern Sierra Nevada, California: a case for extensional tectonics. *Tectonics* **1**, 65–94.

Van Den Eeckhout, G. J. & Vissers, R. 1986. On the role of diapirism in the segregation, ascent and final emplacement of granitoid magmas—Discussion. *Tectonophysics* **127**, 161–169.

Vernon, R. H. 1989. Evidence of syndeformational contact metamorphism from porphyroblast–matrix relationships. *Tectonophysics* **158**, 113–126.

Vissers, R. L. M. 1989. Asymmetric *c*-axis fabrics and flow vorticity: a study using rotated garnets. *J. Struct. Geol.* **11**, 231–244.

Zwart, H. J. 1962. On the deformation of polymetamorphic mineral associations and its application to the Bosost area (Central Pyrenees). *Geol. Rdsch.* **52**, 38–65.